Korean J. Chem. Eng., **31**(12), 2274-2279 (2014)
DOI: 10.1007/s11814-014-0254-5

pISSN: 0256-1115
eISSN: 1975-7220

Etch characteristics of CoFeB thin films and magnetic tunnel junction stacks in a H_2O/CH_3OH plasma

Su Min Hwang, Adrian Garay, Il Hoon Lee, and Chee Won Chung†

Department of Chemistry and Chemical Engineering, Center for Design and Applications of Molecular Catalysts, Inha University, 100 Inha-ro, Nam-gu, Incheon 402-751, Korea
(*Received 26 March 2014 • accepted 28 August 2014*)

Abstract−Inductively coupled plasma reactive ion etching of CoFeB thin films and magnetic tunnel junction (MTJ) stacks with nanometer-sized patterns was performed using H_2O/CH_3OH gas mixture. As the CH_3OH concentration in H_2O/CH_3OH increased, the etch rate of both the CoFeB films and MTJ stacks increased, but the etch selectivity decreased while the etch profiles of CoFeB films and MTJ stacks improved. Field emission transmission electron microscopy observation clearly revealed that the MTJ stacks etched at 75% CH_3OH in H_2O/CH_3OH gas mixture showed a good etch profile without any redeposition and a high degree of anisotropy. These results indicate that there were some chemical reactions between CH_X in H_2O/CH_3OH plasma and the films that comprise the MTJ stacks, such as CoFeB magnetic films. It was confirmed that H_2O/CH_3OH gas mixture could be a good etch gas in attaining a high etch rate and high degree of anisotropy in the etch profile.

Keywords: CoFeB, Magnetic Tunnel Junction Stack, Inductively Coupled Plasma Reactive Ion Etching, H_2O/CH_3OH

INTRODUCTION

To replace conventional dynamic random access memory (DRAM), a variety of new semiconductor memory devices, containing resistive random access memory (ReRAM), phase change random access memory (PCRAM), and magnetic random access memory (MRAM) have been developed. Among these the memory device that has drawn more attention as the next generation memory is the MRAM because of its non-volatility, fast access time, unlimited read/write endurance, low operating voltage, and high storage density [1].

The MRAM, which is operated by tunneling magneto resistance (TMR) effect, has been studied by many research groups, along with the discovery of the spin transfer torque effect [2-4]. The MRAM device is basically composed of a magnetic tunnel junction (MTJ) stack and a complementary metal-oxide semiconductor (CMOS). Because the etching process of MTJ stacks is one of the key processes for the fabrication of high-density MRAM, dry etching of MTJ stacks should be developed. However, dry etching of MTJ stacks has revealed to be extremely difficult, because the metals and magnetic materials in MTJ stacks rarely react with the chemically reactive species produced in the plasma. As the critical dimensions of MTJ stacks diminish, the importance of the etching process increases.

To overcome this difficulty, many dry etching methods have been employed to etch MTJ stacks as well as various magnetic thin films including CoFeB films. Primarily, ion beam etching was used to etch magnetic films and MTJ stacks, but it exhibited unsuitable features such as slow etch rate, sidewall redeposition, and etching damage due to the physical sputtering etching mechanism [5,6]. On the pursuit of developing a better dry etching process chemically assisted ion beam etching, which induces chemical reactions during the etching process, was employed to etch magnetic films and MTJ stacks; but the results showed little improvement over ion beam etching [7,8]. To further improve the etch characteristics of magnetic films, eventually, reactive ion etching (RIE) was introduced. Chlorine-containing gases such as Cl_2 and BCl_3 were initially used to etch the magnetic films, but nonvolatile etching byproducts remained on the sidewall of the films. In addition, the etch residues consisted of chlorine compounds, which caused the surface to corrode after etching [9-11]. As an alternative, the etching of magnetic films and MTJ stacks was performed using HBr/Ar plasma, but an etch profile with a slanted etch slope was obtained [12,13]. Recently, to avoid this problem while improving the etch characteristics, inductively coupled plasma reactive ion etching (ICPRIE) was employed to etch magnetic films and MTJ stacks using noncorrosive etching gases such as CO/NH_3, CH_3OH/Ar and $CH_4/O_2/Ar$ [14-18]. In particular, when CH_3OH and CH_4/O_2 gases were used, the etch profiles of CoFeB film and MTJ stacks showed significant improvement. However, the etching results of MTJ stacks with nanometer size patterns are still inadequate to be for use in high density MRAM devices.

We investigated the etch characteristics of CoFeB magnetic thin films and MTJ stacks with nanometer-sized patterns using an ICPRIE system. Our previous study proved that the etching of magnetic materials using H_2O gas was very effective and CH_3OH gas also showed good etch characteristics on the films [17,19-21]. Therefore, the H_2O/CH_3OH gas mixture was applied to etch the CoFeB films and MTJ stacks. Field emission scanning electron microscopy (FESEM) was used to observe the etch profiles. For more detailed observation of the etch profiles and plasma analysis, field emission transmission electron microscopy (FETEM) and optical emission spectroscopy (OES) were used, respectively.

†To whom correspondence should be addressed.
E-mail: cwchung@inha.ac.kr

EXPERIMENTAL DETAILS

The structure of MTJ stacks used in this study is as follow: W(70)/TiN(100)/Ru(5)/CoFeB(2)/MgO(0.8)/CoFeB(1.5)/Ru(0.8)/CoFe(1.5)/PtMn(15)/TiN(45)/oxide/Si substrate (nm in unit). W and TiN double layers were used as a hard mask which had the thicknesses of 70 nm and 100 nm, respectively, and the MgO thin film was employed as a tunneling barrier layer. All of the layers were deposited on an SiO_2/Si substrate by direct-current (dc) magnetron sputtering. The hard mask layers which were deposited on the top of the MTJ stacks were patterned by e-beam lithography using a negative electron (e)-beam resist of 300 nm, and then etched by ICPRIE using a Cl_2/C_2F_6/Ar gas. Finally, the patterns on MTJ stacks which consisted of 90×90 nm^2 square arrays with a space of 90 nm were prepared [17,18]. CoFeB magnetic thin films with a thickness of 100 nm were prepared on Si substrates and TiN masks were deposited on top of CoFeB films using dc sputtering method. Patterned TiN/CoFeB films with parallel lines of different thickness were prepared by ICPRIE etching using a Cl_2/C_2F_6/Ar gas after a conventional photolithography.

An ICPRIE system (A-Tech System, Korea), which was equipped with a main chamber and a load lock chamber, was used to etch CoFeB films and the MTJ stacks using H_2O/CH_3OH gas mixture. Helium backside cooling system was used to cool the substrate. The susceptor was chilled by a cold fluid at 12-15 ºC through a circulator. The main coil was connected to a 13.56 MHz rf power supply to generate a high density plasma. A dc-bias voltage was induced by another rf power at 13.56 MHz which was coupled to the substrate susceptor to control the ion energy in the plasma. The liquid H_2O and CH_3OH sources were evaporated by two vaporizers and fed into the etch chamber. The flow rates of these two vapors were controlled by two exclusive mass flow controllers.

We investigated the etch characteristics of CoFeB films and MTJ stacks by varying CH_3OH concentrations in H_2O/CH_3OH gas mixture. The etch profiles were observed by FESEM (Hitachi; S-4300SE) at an operating voltage of 20 kV. To observe the etch profiles more clearly, FETEM (JEOL; JEM-2100F) of an operating voltage of 200 kV was employed. The samples for FETEM analysis were prepared by the conventional dimpler, polisher and precision ion polisher system (PIPS) (GATAN; 691). The redeposition of the etched MTJ stacks was identified by FETEM. The OES (Ocean Optics; Maya 2000 pro) was used to analyze active species in H_2O/CH_3OH plasmas to understand the etch mechanism involved in the etching of CoFeB thin films.

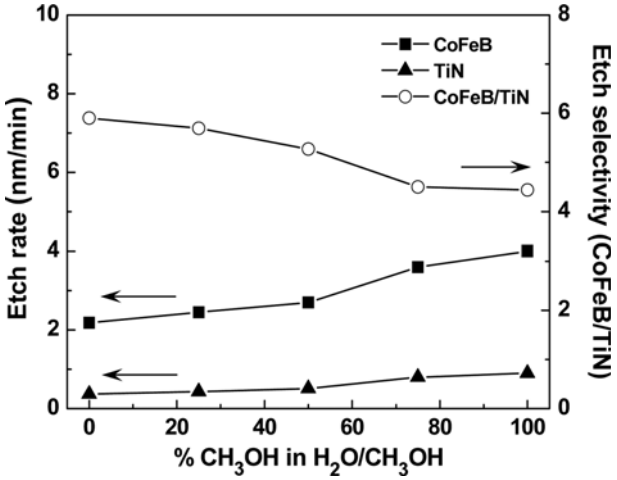

Fig. 1. Etch rates of CoFeB thin films and TiN masks and etch selectivity of CoFeB to TiN for various CH_3OH concentrations in an H_2O/CH_3OH gas mixture. Etch conditions: 800 W ICP power, 300 V dc-bias voltage and 5 mTorr gas pressure.

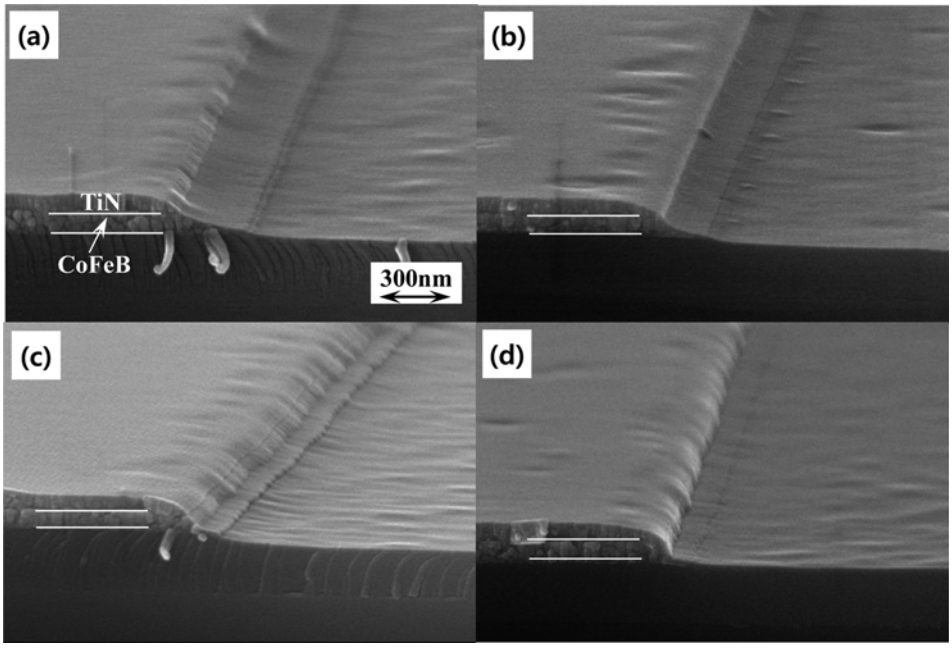

Fig. 2. FESEM micrographs of CoFeB thin films etched in various CH_3OH concentrations in a H_2O/CH_3OH gas mixture. (a) 100% H_2O, (b) 25% CH_3OH/H_2O, (c) 50% CH_3OH/H_2O, (d) 75% CH_3OH/H_2O; Etch conditions: 800 W ICP power, 300 V dc-bias voltage and 5 mTorr gas pressure.

RESULTS AND DISCUSSION

Fig. 1 shows the etch rates of both CoFeB thin films and TiN masks, and the etch selectivity of CoFeB to TiN for various CH_3OH concentrations in H_2O/CH_3OH gas mixture. The etch conditions were as follows: ICP power of 800 W, dc-bias voltage of 300 V and a gas pressure of 5 mTorr. As the CH_3OH concentration increased in H_2O/CH_3OH gas mix, the etch rates of CoFeB films and TiN increased. These results indicated that CH_x species in CH_3OH plasma contributed to enhance the etch rates of the films by some chemical reactions. However, the etch selectivity of CoFeB films to TiN mask decreased with increasing CH_3OH concentration due to the increase in etch rate of TiN mask. It seems to be an optimal CH_3OH concentration in H_2O/CH_3OH gas mix.

Fig. 2 shows the FESEM micrographs of CoFeB thin films etched in various CH_3OH concentrations of H_2O/CH_3OH gas mixture. Fig. 2(a) shows the etch profile of CoFeB films etched in H_2O gas only. As can be seen, the etch slope (the sidewall angle of the etched films) of CoFeB films was very slanted. As the CH_3OH gas was added to H_2O gas, the etch profiles of CoFeB films were improved. The best etch profiles could be observed at the etch condition of 75% CH_3OH. Therefore, it appears that CH_3OH gas has positive effects on the etching of CoFeB thin films.

Fig. 3 shows the etch rates of MTJ stacks and hard masks as well as the etch selectivity of MTJ stacks to hard mask for various CH_3OH concentrations in H_2O/CH_3OH gas mixture. The etch condition was the same as that of CoFeB etching. As the CH_3OH concentration in H_2O/CH_3OH gas mixture increased, the etch rates of the MTJ stacks and the hard masks gradually increased, while the etch selectivity of the MTJ stacks slightly decreased. Generally, the etch rate is increased by direct sputtering over the film and/or the chemical reaction between the etching gas and the elements that constitute

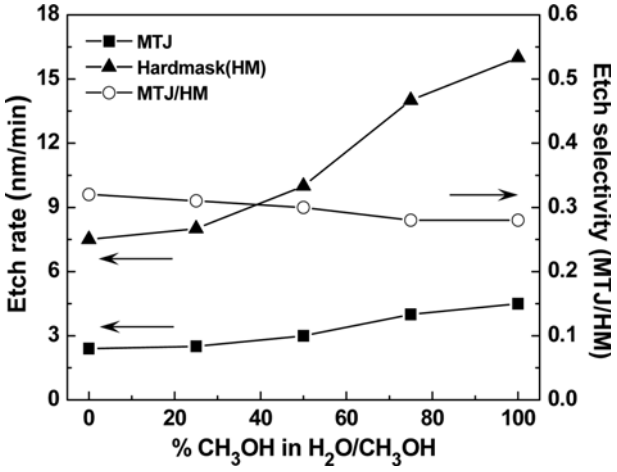

Fig. 3. Etch rates of MTJ stacks and hard masks and etch selectivity of MTJ stacks to hard mask for various CH_3OH concentrations in a H_2O/CH_3OH gas mixture. Etch conditions: 800 W ICP power, 300 V dc-bias voltage and 5 mTorr gas pressure.

the film. From the etch rate and etch selectivity results, the addition of CH_3OH in H_2O gas enhanced the chemical reactions between the radicals (CH_x) in CH_3OH plasma and the various layers in MTJ stacks and/or some sputtering effect of CHx species. These results revealed an inverse relationship between the etch rates of MTJ stacks and the etch selectivity of MTJ stacks to hard mask.

Fig. 4 shows the FESEM micrographs of MTJ stacks etched in different CH_3OH concentrations in H_2O/CH_3OH gas mixture. Fig. 4(a) shows the etch profile of MTJ stacks etched in 100% H_2O gas. The MTJ stacks were 90×90 nm^2 square and were formed as an array with 90 nm space intervals between stacks. The space between

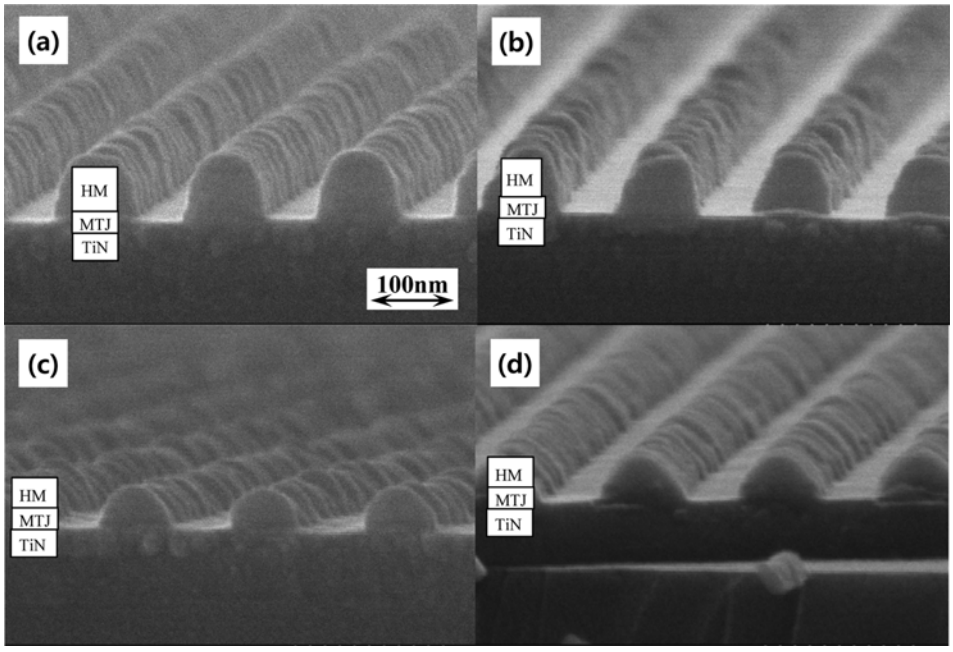

Fig. 4. FESEM micrographs of MTJ stacks etched in various CH_3OH concentrations in an H_2O/CH_3OH gas mixture. (a) 100% H_2O, (b) 25% CH_3OH/H_2O, (c) 50% CH_3OH/H_2O, (d) 75% CH_3OH/H_2O; Etch conditions: 800 W ICP power, 300 V dc-bias voltage and 5 mTorr gas pressure.

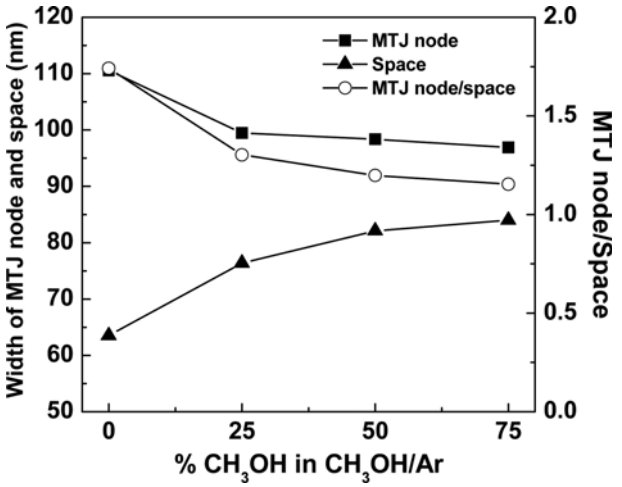

Fig. 5. Change in width of MTJ stacks and space after etching in various CH_3OH concentrations in an H_2O/CH_3OH gas mixture. Etch conditions: 800 W ICP power, 300 V dc-bias voltage and 5 mTorr gas pressure.

MTJ stacks after etching became narrower compared to the pattern before etching, which means that there were some redeposited materials on the sidewall of the MTJ stacks. However, the redeposition on the sidewall could not be exactly identified from the SEM images, and the etch slope of the MTJ stacks appeared to be relatively vertical. Therefore, it needed to be verified by TEM analysis for clear observation. As the CH_3OH gas concentration increased relative to H_2O gas, the height of hard masks in MTJ stacks seemed to decrease and it was uncertain that the etch profiles improved as shown in Fig. 4(b). However, in the cases of 50% and 75% CH_3OH in H_2O/CH_3OH gas mixture (Figs. 4(c) and 4(d)), the space between the MTJ stacks became wider, similar to that of MTJ stacks before etching. Fig. 5 shows the changes in width of MTJ stacks and space after etching at different CH_3OH/Ar gas ratios. Each value was measured from Fig. 4 and the results can be considered to be relative comparison. As the CH_3OH concentration increased, the etched MTJ nodes became narrow, whereas the space became wider. In addition, the ratio of the width of MTJ node to space was close to 1 due to the change in the width of MTJ node and space with increasing CH_3OH concentration. It suggests that the redeposition on the sidewall of MTJ stacks was reduced on these etch conditions. It is predicted that the etching of MTJ stacks in H_2O/CH_3OH gas mixture proceeds with some chemical reactions and minor redeposition on the sidewall of the MTJ stacks.

To improve the etch profile of MTJ stacks further, the evolution of the etch profile for a variation of etching time at 75% CH_3OH in CH_3OH/H_2O gas mixture was studied while the other parameters applied during the etching process were kept fixed at ICP power of 900 W, dc-bias voltage of 300 V and a gas pressure of 1 mTorr. Fig. 6 shows FESEM images of the MTJ depicting the evolution of the etch profile as a function of etching time, while remaining etch conditions fixed as described above. When the MTJ stacks were etched for 6 min, the space between the MTJ stacks became narrower, suggesting that a slight amount of redeposition was formed on the MTJ stack sidewalls (Fig. 6(a)). However, as the etching proceeded further, the space between nodes (MTJ stacks) became wider and the

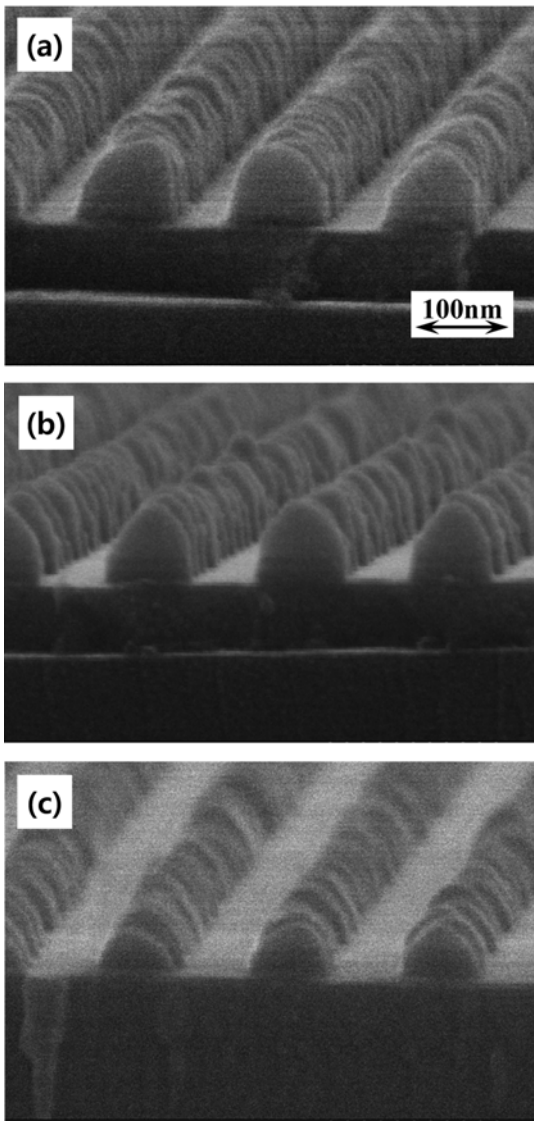

Fig. 6. FESEM micrographs of MTJ stacks etched at different etching times: (a) 6 min, (b) 7 min and (c) 8 min. Etch conditions: 75% CH_3OH/H_2O gas mixture, 900 W ICP power, 300 V dc-bias voltage and 1 mTorr gas pressure.

redeposition on the sidewall seemed to decrease, as shown in Fig. 6(b). Finally, as depicted by Fig. 6(c), the etch profile after the etching time for 8 min shows that the level of redeposition decreased significantly, resulting in better separation between nodes (MTJ stacks). Based on the etch results in Fig. 6, the relative changes in the width of MTJ stacks and space were plotted in Fig. 7. With increase of etching time, the width of MTJ stacks decreased, while the space between MTJ nodes became wider. The evolution of etch profile of MTJ stacks reveals the etch mechanism of MTJ stacks in H_2O/CH_3OH gas mixture. At early stage of etching, the etch-byproducts by the chemical reaction of etch gas with the films of the MTJ stacks and/or by sputtering were formed on the sidewall of the MTJ stacks, resulting in the narrow spaces of the MTJ stacks. However, as the etching proceeded, the etch-byproducts on the sidewall of the MTJ stack could be sputtered-off, leading to the wide space of the MTJ stacks. Therefore, the addition of 75% CH_3OH in H_2O at these condi-

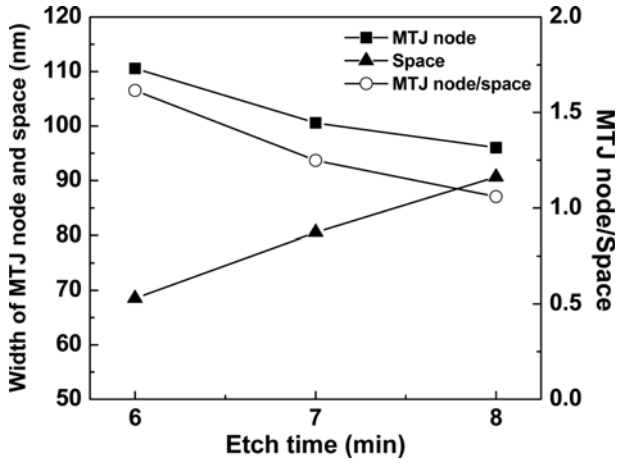

Fig. 7. Change in width of MTJ stacks and space after etching at different etching times. Etch conditions: 800 W ICP power, 300 V dc-bias voltage and 5 mTorr gas pressure.

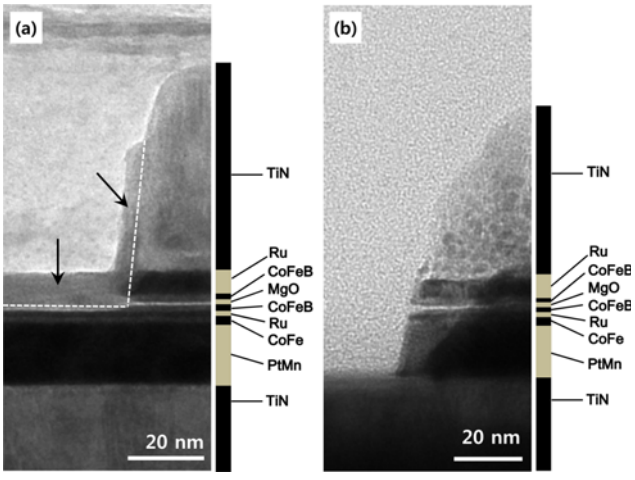

Fig. 8. TEM micrographs of the MTJ stacks etched in (a) 100% H_2O gas (Etch conditions: 800 W ICP power, 300 V dc-bias and 5 mTorr gas pressure), and (b) 75% CH_3OH in a H_2O/CH_3OH gas mixture (Etch conditions: 900 W ICP power, 300 V dc-bias voltage and 1 mTorr gas pressure).

tions revealed to aid in improving etch rate and etch profile of MTJ stacks.

To obtain a clearer verification of the etch profile of MTJ stacks and possible redeposition on the sidewalls and etched surface, the MTJ stacks were observed by FETEM. Fig. 8(a) shows the etch profile of the MTJ stacks etched in 100% H_2O gas, which was the same specimen observed in Fig. 4(a). A relatively good profile was expected to be obtained from the SEM observation of Fig. 4(a), but the TEM observation clearly revealed heavy redeposition on both the etched surface and the sidewall of the MTJ stacks (marked with white dotted line and black arrows). It was identified that the redeposited materials were composed of various metals (Ru, Co, Fe, Pt, Mn and Ti) generated from the MTJ stacks and O originated from the epoxy used during the specimen preparation for the TEM analysis. Also, it was determined that the etching was disrupted on the lower Ru layer due to the formation of heavy redeposition during the etching. It can be concluded that 100% H_2O was not suitable to

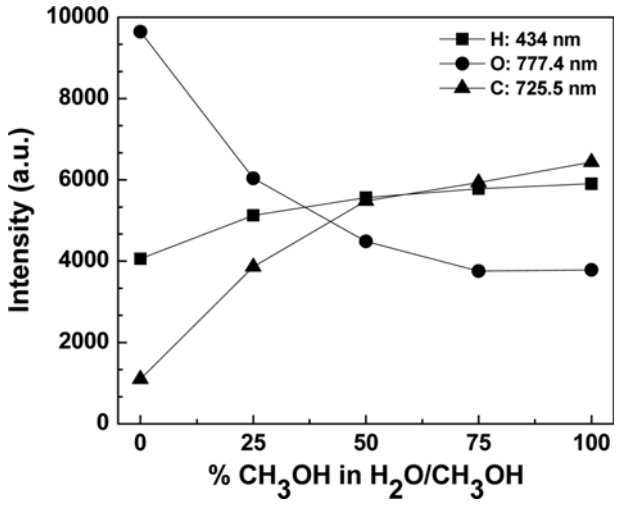

Fig. 9. OES analysis of plasmas for various CH_3OH concentrations in an H_2O/CH_3OH gas mixture. Plasma conditions: 800 W ICP power, 300 V dc-bias voltage and 5 mTorr gas pressure.

etch the MTJ stacks. On the other hand, Fig. 8(b) shows the etch profile of the MTJ stacks etched in 75% CH_3OH/H_2O gas mixture at 900 W ICP power, 300 V dc-bias voltage and 1 mTorr gas pressure. We verified that the MTJ stacks were etched down to the TiN bottom electrode. In addition, TEM observation revealed that the hard mask after etching remained on top of MTJ stacks. The TEM image clearly shows that there was no redeposition or etch residues, neither on the sidewall nor on the surface of the MTJ stacks. Therefore, it is safe to conclude that the addition of CH_3OH gas in H_2O gas effectively aided in achieving a good etch profile without the redeposition on the sidewall of the MTJ stacks.

Fig. 9 shows the OES analysis of plasmas in various CH_3OH concentrations of H_2O/CH_3OH gas mixture. Plasma conditions were 800 W ICP power, 300 V dc-bias voltage and 5 mTorr gas pressure. Hydrogen, oxygen and carbon were analyzed and the selected wavelengths for each element were 434, 777.4 and 725.5 nm, respectively. As the CH_3OH gas in H_2O/CH_3OH gas mixture increased, the intensities of carbon and hydrogen increased while the intensity of oxygen decreased. When the etch profiles shown in Fig. 4 are compared with the results of OES analysis, the increase of carbon and hydrogen peaks might be responsible for the improved etch profile. Especially, the increase of carbon peak played an important role in decreasing the redeposited materials on the sidewall of the patterns, forming C, CHx and O containing metal compounds which could be sputtered off easily. The gradual increase of hydrogen peak meant the increase in degree of anisotropy in etch profile, forming the protecting layers containing CHx or OH on the films, especially on the pattern sidewall. These facts could be confirmed by individual etching studies of each film forming the MTJ stacks. As a result, the role of CHx in CH_3OH gas is a key point in achieving good etch profile of MTJ stacks.

CONCLUSION

CoFeB thin films and MTJ stacks with nanometer size patterns were etched by using H_2O/CH_3OH gas mixture. The etch rates of

CoFeB films, TiN mask and MTJ stacks, and the etch selectivities of CoFeB and MTJ to hard mask were obtained in various CH_3OH concentrations of H_2O/CH_3OH gas mixture. As the CH_3OH concentration increased, the etch rate of both the CoFeB films and TiN masks increased while the etch selectivity decreased. These results imply that the addition of CH_3OH gas in H_2O gas enhanced some chemical reactions between CH_x species in CH_3OH plasma and CoFeB films and/or sputtering by CHx species. The etch profiles of CoFeB films in various CH_3OH concentrations revealed that 75% CH_3OH was the optimal etching gas concentration. At this etch condition, a good etch profile with high degree of anisotropy without the redeposition or etch residues was obtained.

For the etching of MTJ stacks, as the CH_3OH gas was added to H_2O gas, the etch rate of MTJ and hard mask increased, but the etch selectivity of MTJ to hard mask decreased. So the CH_3OH concentration in H_2O/CH_3OH mixture should be optimized to obtain good etch characteristics of MTJ stacks. As the CH_3OH concentration in H_2O/CH_3OH increased, the space between the etched MTJ stacks became wider, indicating that the redeposition on the sidewall decreased. The observation on the evolution of the etch profile at different etching times enables us to elucidate the etch mechanism under H_2O/CH_3OH gas chemistry. Initially, the etching of MTJ stacks appeared to proceed by physical sputtering and/or by forming non-volatile etch byproducts, but as the etching proceeded, the space between the MTJ stacks became wider. It was thought that the decrease of etch redeposition was attributed to easy sputter-off of the redeposited materials on the sidewall, which were formed at early stages of the MTJ stacks etching. These redeposited materials were formed by the chemical reactions between the high CH_3OH concentrations (75%) and the different metallic films of which the MTJ stacks are composed.

TEM observation revealed that the MTJ stacks etched in 100% H_2O produced heavy redeposition on the sidewall of the MTJ stacks and on the surface of the lower Ru layer. These were attributed to the formation of non-volatile compounds during the etching. On the other hand, when the MTJ stacks were etched in 75% CH_3OH of H_2O/CH_3OH gas mixture, good etch profile with a high degree of anisotropy without any redepositions was achieved. We verified that the H_2O/CH_3OH gas mixture could be a good etch gas in accomplishing high degree of anisotropy in the etch profiles of CoFeB films and MTJ stacks.

ACKNOWLEDGEMENTS

This research was supported by a grant from the R&D Program for Industrial Core Technology funded by the Ministry of Trade, Industry and Energy (MOTIE), Republic of Korea (Grant No. 10044723). This work was supported by an INHA UNIVERSITY Research Grant.

REFERENCES

1. J. M. Slaughter, R. W. Dave, M. DeHerrera, M. Durlam, B. N. Engel, J. Janesky, N. D. Rizzo and S. Tehrani, *Journal of Superconductivity: Incorporating Novel Magnetism*, **15**, 19 (2002).
2. S. A. Wolf, J. Lu, M. R. Stan, E. Chen and D. M. Treger, *Proc. IEEE*, **98**, 2155 (2010).
3. T. Miyazaki, S. Kumagai and T. Yaoi, *J. Appl. Phys*., **81**, 3753 (1997).
4. J. A. Katine and E. E. Fullerton, *J. Magn. Magn. Mater*., **320**, 1217 (2008).
5. S. J. Pearton, C. R. Abernathy, F. Ren and J. R. Lothian, *J. Appl. Phys*., **76**, 1210 (1994).
6. R. C. Sousa and P. P. Freitas, *IEEE Trans. Magn*., **37**, 1973 (2001).
7. M. J. Vasile and C. J. Mogab, *J. Vac. Sci. Technol. A*, **4**, 1841 (1986).
8. J. D. Chinn, I. Adesida and E. D. Wolf, *J. Vac. Sci. Technol. B*, **1**, 1028 (1983).
9. S. R. Min, H. N. Cho, K. W. Kim, Y. J. Cho, S. H. Choa and C. W. Chung, *Thin Solid Films*, **516**, 3507 (2008).
10. K. B. Jung, E. S. Lambers, J. R. Childress, S. J. Pearton, M. Jenson and A. T. Hurst, Jr., *Appl. Phys. Lett*., **71**, 1255 (1997).
11. I. K. Park, S.R. Min, W. H. Park, K. H. Shin and C. W. Chung, *J. Magn. Magn. Mater*., **304**, e264 (2006).
12. S. R. Min, H. N. Cho, S. J. Noh, K. W. Kim, S. A. Seo and C. W. Chung, *Phys. Stat. Sol. (c)*, **4**, 4416 (2007).
13. E. H. Kim, Y. B. Xiao, S. M. Kong and C. W. Chung, *J. Nanosci. Nanotechnol*., **11**, 6616 (2011).
14. N. Matsui, K. Mashimo, A. Egami, A. Konishi, O. Okada and T. Tsukada, *Vacuum*, **66**, 479 (2002).
15. X. Kong, D. Krsa, H. P. Zhou, W. Williams, S. McVitie, J. M. R. Weaver and C. D. W. Wilkinson, *Microelectron. Eng*., **85**, 988 (2008).
16. Y. Otani, H. Kubota, A. Fukushima, H. Maehara, T. Osada, S. Yuasa and K. Ando, *IEEE Trans. Magn*., **43**, 2776 (2007).
17. E. H. Kim, T. Y. Lee and C. W. Chung, *J. Electrochem. Soc*., **159**, H230 (2012).
18. T. Y. Lee, E. H. Kim, I. H. Lee and C. W. Chung, *ECS J. Solid State Sci. Technol*., **1**, P233 (2012).
19. Y. B. Xiao, E. H. Kim, S. M. Kong and C. W. Chung, *Thin Solid Films*, **519**, 6673 (2011).
20. I. H. Lee, T. Y. Lee and C. W. Chung, *Microelectron. Eng*., **108**, 39 (2013).
21. I. H. Lee, T. Y. Lee and C. W. Chung, *Vacuum*, **97**, 49 (2013).